

Supplementary Information

Machine Learning-Enabled Planar Interdigitated Thermogalvanic Hydrogel for Synergistic Thermal and Strain Sensing

Qi Hu¹, Hao Wu², Chunxuan Yu¹, Hao Xiao¹, Chen Shen¹, Zhaoquan Zhao¹, Yuan Yao¹, Xuelin Yong², Xing Liang³, Hongwei Wu⁴, Xiaoze Du¹, Cheng Chi^{1,4*}

¹Key Laboratory of Power Station Energy Transfer Conversion and System of Ministry of Education, School of Energy Power and Mechanical Engineering, North China Electric Power University, Beijing, 102206, China

² School of Mathematics and Physics, North China Electric Power University, Beijing, 102206, China

³School of Computer Science and Mathematics, Kingston University London, KT1 2EE, United Kingdom

⁴School of Physics, Engineering and Computer Science, University of Hertfordshire, Hatfield AL10 9AB, United Kingdom

*Corresponding Author: chicheng@ncepu.edu.cn

Inventory of Supplementary Information:

Supplementary Figures and tables

Supplementary Fig. S1 **Photograph of the MXene electrode directly printed on a polyimide (PI) substrate.**

Supplementary Fig. S2 **Adhesion test of the MXene electrode on the PET substrate using the tape-peeling method.**

Supplementary Fig. S3 **Ti 2p XPS spectra of MXene electrodes immediately after printing and after ambient storage for three days.**

Supplementary Fig. S4 **FTIR spectra of pure PAAm hydrogel and PAAm hydrogel containing redox ion pairs.**

Supplementary Fig. S5 **EIS spectra of the device at 0, 1, and 6 h. (b) EIS spectrum at 12 h.**

Supplementary Fig. S6 **Time-dependent voltage response to various temperature gradients for (a) freshly prepared and (b) after 8 hours of ambient exposed PITH device. Thermopower fitting of the PITH device: (c) freshly prepared device and (d) device after 8 h of ambient exposure.**

Supplementary Fig. S7 **Photograph of the fully dehydrated PITH device after storage under ambient conditions for four days.**

Supplementary Fig. S8 **(a) Photograph of the electrical conductivity measurement using a four-point probe. (b) Variation of the electrical resistance (R) of the MXene electrode as a function of bending cycles.**

Supplementary Fig. S9 **Boxplot of voltage responses of the PITH under transient touch and prolonged touch.**

Supplementary Fig. S10 **Photographs demonstrating the PITH device attached to a gloved finger during the handwriting of different letters.**

Supplementary Fig. S11 **Voltage response curves of handwritten digit “0” under (a) no-temperature-gradient and (b) temperature-gradient**

conditions. (c) Comparison of recognition accuracies for digit handwriting with and without a temperature gradient.

Supplementary Table S1 Resistance of the printed MXene electrodes under different bending cycles.

Supplementary Table S2 Comparison of the sensing performance between our PITH device and previously reported self-powered thermogalvanic sensors.

Video S1. Direct ink writing (DIW) printing process of interdigital MXene electrodes on a flexible PET substrate, demonstrating the continuous extrusion and pattern fidelity of the MXene ink during electrode fabrication.

Video S2. Appearance and fluidity of the MXene ink, illustrating its homogeneous dispersion and suitable rheological properties for direct ink writing.

Video S3. Manual stretching and mechanical deformation of the PAAm hydrogel, demonstrating its high flexibility, elasticity, and mechanical robustness under tensile strain.

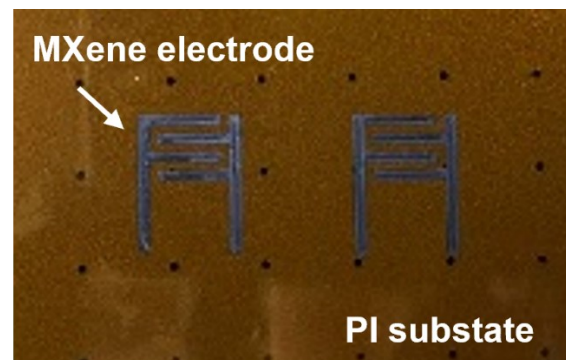


Figure S1. Photograph of the MXene electrode directly printed on a polyimide (PI) substrate.

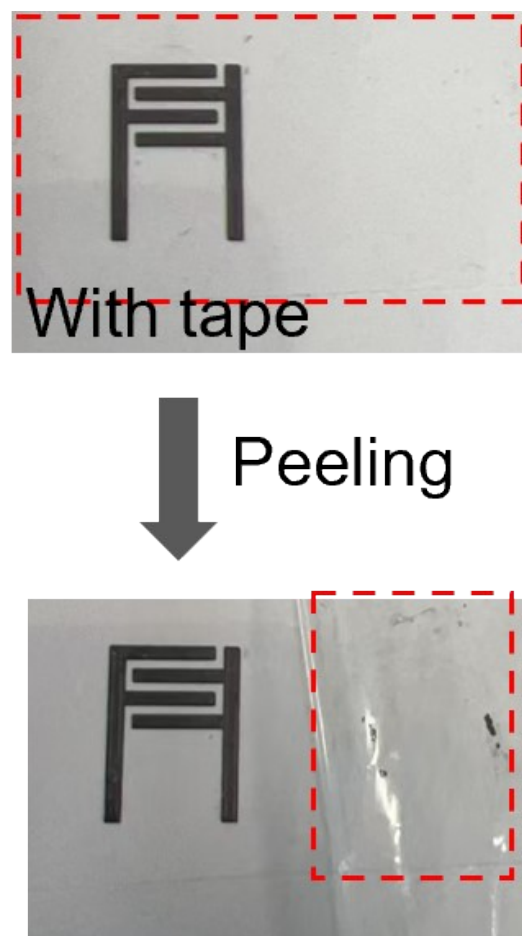


Figure S2. Adhesion test of the MXene electrode on the PET substrate using the tape-peeling method.

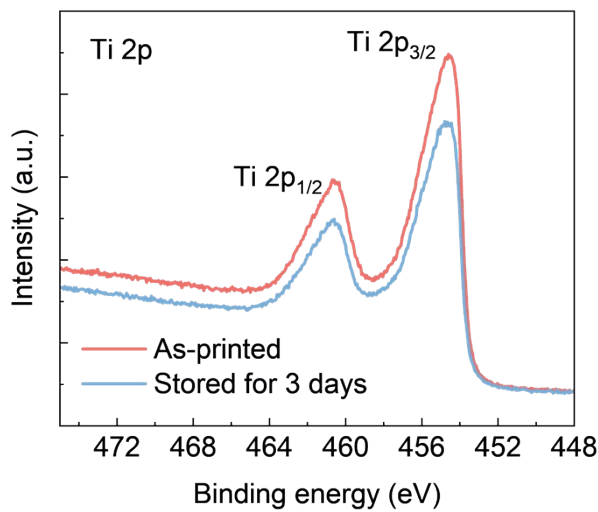


Figure S3. Ti 2p XPS spectra of MXene electrodes immediately after printing and after ambient storage for three days.

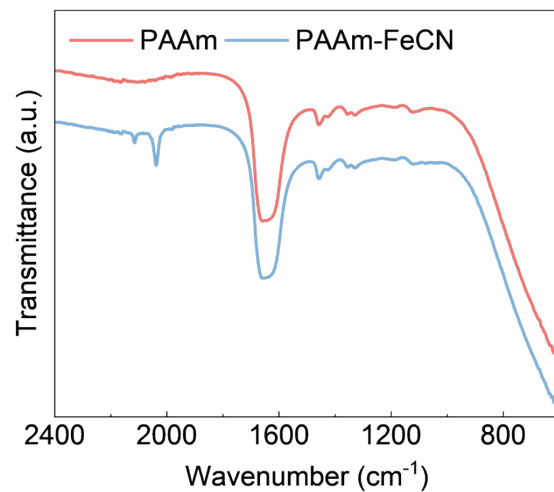


Figure S4. FTIR spectra of pure PAAm hydrogel and PAAm hydrogel containing redox ion pairs.

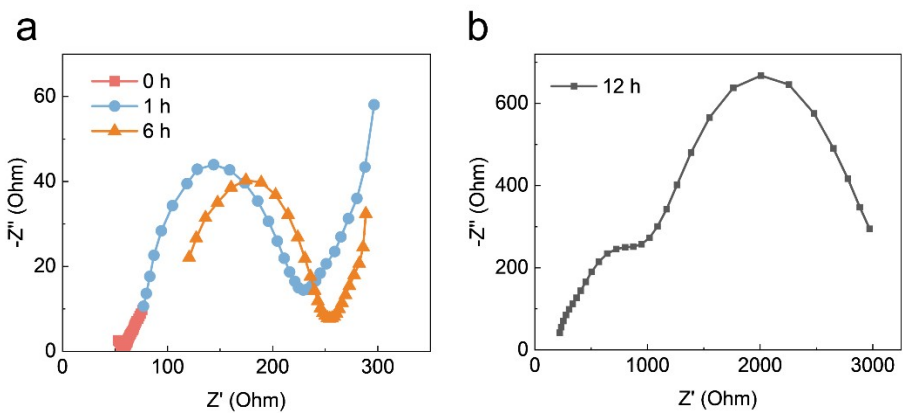


Figure S5. EIS spectra of the device at 0, 1, and 6 h. (b) EIS spectrum at 12 h.

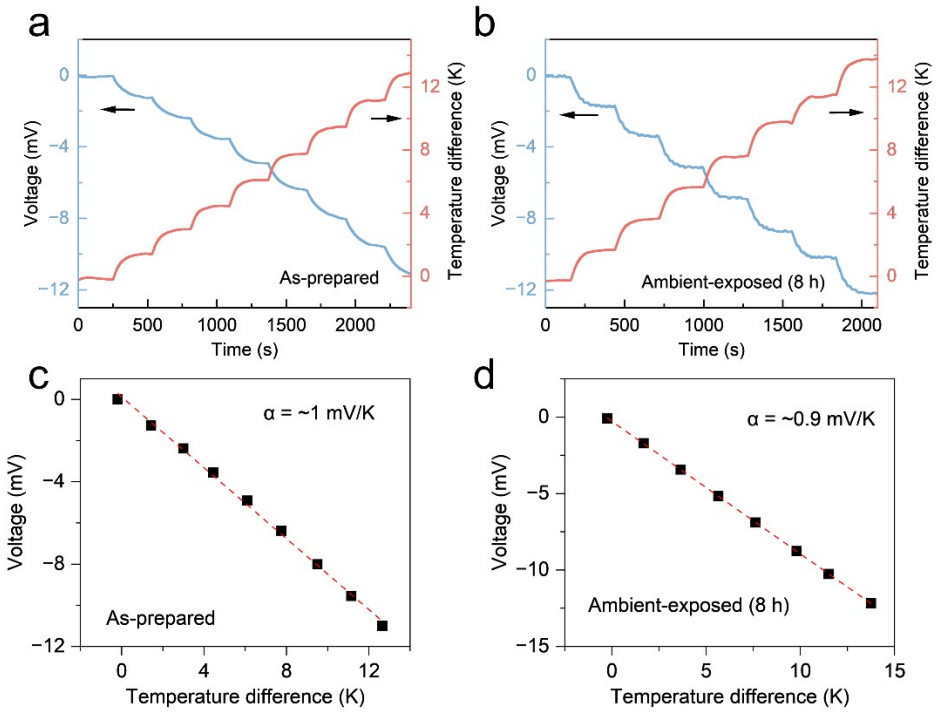


Figure S6. Time-dependent voltage response to various temperature gradients for (a) freshly prepared and (b) after 8 hours of ambient exposed PITH device. Thermopower fitting of the PITH device: (c) freshly prepared device and (d) device after 8 h of ambient exposure.

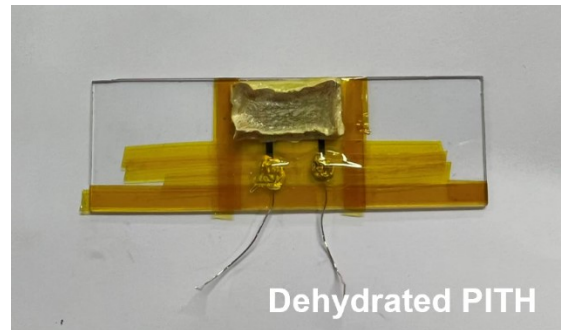


Figure S7. Photograph of the fully dehydrated PITH device after storage under ambient conditions for four days.

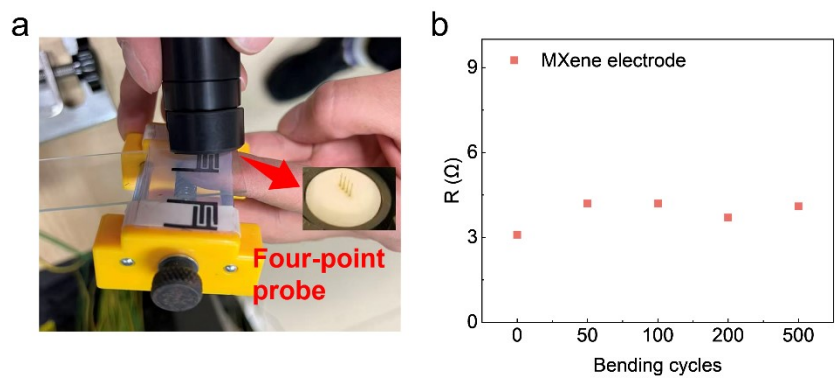


Figure S8. (a) Photograph of the electrical conductivity measurement using a four-point probe. (b) Variation of the electrical resistance (R) of the MXene electrode as a function of bending cycles.

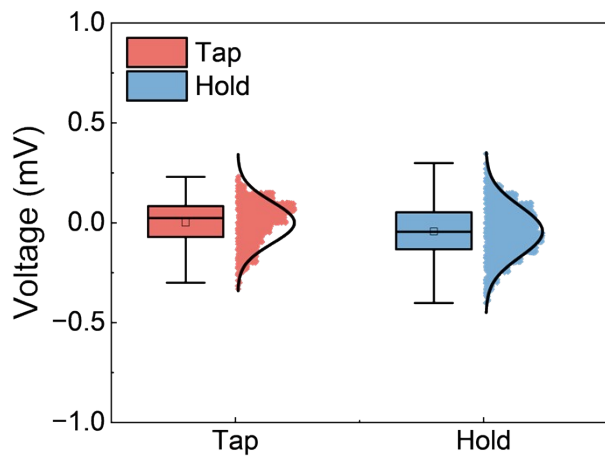


Figure S9. Boxplot of voltage responses of the PITH under transient touch and prolonged touch.



Figure S10. Photographs demonstrating the PITH device attached to a gloved finger during the handwriting of different letters.

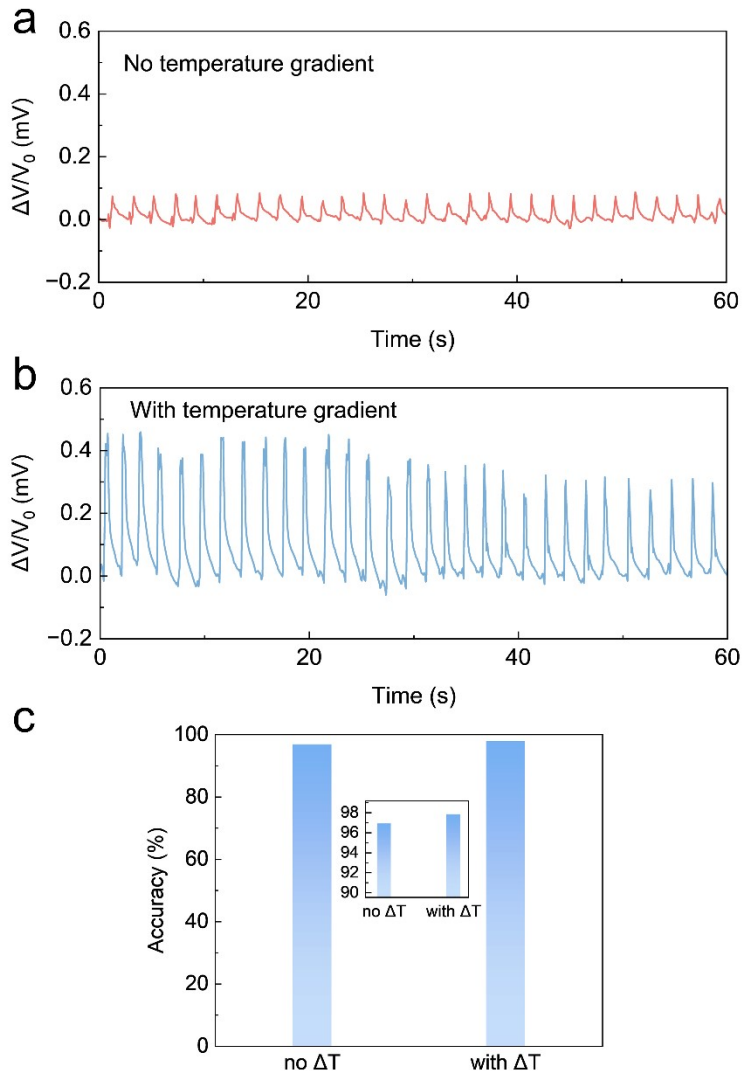


Figure S11. Voltage response curves of handwritten digit “0” under (a) no-temperature-gradient and (b) temperature-gradient conditions. (c) Comparison of recognition accuracies for digit handwriting with and without a temperature gradient.

Table S1. Resistance of the printed MXene electrodes under different bending cycles.

Bending cycles	R (Ω)	σ (S cm $^{-1}$)
0	3.1	2932.6
50	4.2	2164.5
100	4.2	2164.5
200	3.7	2457.0
500	4.1	2217.3

Table S2. Comparison of the sensing performance between our PITH device and previously reported self-powered thermogalvanic sensors.

Device	Materials	Sensing modality	Device configuration	Response time (ms)	thermopower (mV K ⁻¹)	Ref.
Gel Patch	PVA/PDMS + Fe ^{2+/3+}	Photo-thermal-electric	Flexible PTE gel patch	500	1.46	¹
Antifreezing Gel	PVA/EG + Fe(CN) ₆ ^{3-/4-}	Thermal energy harvesting	Sandwich structure	N/A	1.43	²
Fingertip Receptor	PVA + Fe(CN) ₆ ^{3-/4-}	Pressure & Thermal	Micropatterned and gradient structure	80	1.89	³
TGH E-Skin	PAM + LiCl + Fe(CN) ₆ ^{3-/4-}	Thermal (Signature)	Sandwich structure	230	1.82	⁴
Smart Pen	PVA/Gelatin + Fe(CN) ₆ ^{3-/4-}	Thermal & Piezoresistive	Gel-wrapped pen structure	130	2.05	⁵
TGH Array	PVA/Agar + Fe(CN) ₆ ^{3-/4-}	Thermal (Biometric)	Concave-arranged array	N/A	1.50	⁶
PITH	PAAm + Fe(CN) ₆ ^{3-/4-}	Thermal-strain coupled	Planar interdigitated	390	1.44	This work

*The corresponding full name for abbreviation in the table as follows.

PVA: poly(vinyl alcohol), PDMS: polydimethylsiloxane, EG: ethylene glycol, PAM: polyacrylamide, TGH: thermogalvanic hydrogel

References

(1) Yang, H.; Ahmed Khan, S.; Li, N.; Fang, R.; Huang, Z.; Zhang, H. Thermogalvanic gel patch for self-powered human motion recognition enabled by photo-thermal-electric conversion. *Chem. Eng. J.* 2023, *473*, 145247.

(2) Zhang, D.; Zhou, Y.; Mao, Y.; Li, Q.; Liu, L.; Bai, P.; Ma, R. Highly antifreezing thermogalvanic hydrogels for human heat harvesting in ultralow temperature environments. *Nano Lett.* 2023, *23* (23), 11272-11279.

(3) Li, N.; Wang, Z.; Niu, Y.; Li, Y.; Wen, S.; Zhang, H.; Lin, Z. H. Bionic Multimodal Augmented Somatosensory Receptor Enabled by Thermogalvanic Hydrogel. *Adv. Sci.* 2025, e05873.

(4) Li, N.; Wang, Z.; Yang, X.; Zhang, Z.; Zhang, W.; Sang, S.; Zhang, H. Deep - learning - assisted thermogalvanic hydrogel e - skin for self - powered signature recognition and biometric authentication. *Adv. Funct. Mater.* 2024, *34* (18), 2314419.

(5) Sang, S.; Bai, C.; Wang, W.; Khan, S. A.; Wang, Z.; Yang, X.; Zhang, Z.; Zhang, H. Finger temperature-driven thermogalvanic gel-based smart pen: Utilized for identity recognition, stroke analysis, and grip posture assessment. *Nano Energy* 2024, *123*, 109366.

(6) Zhang, D.; Xu, Z.; Wang, Z.; Cai, H.; Wang, J.; Li, K. Machine-learning-assisted wearable PVA/Acrylic fluorescent layer-based triboelectric sensor for motion, gait and individual recognition. *Chem. Eng. J.* 2023, *478*, 147075.